

Origin of copper as a unique catalyst for C–C coupling in electrocatalytic CO₂ reduction

Jie Chen,^{abc} Benjamin W. J. Chen,^d Jia Zhang,^{*d} Wei Chen,^{abe} and Yi-Yang Sun^{*c}

a. Joint School of National University of Singapore and Tianjin University, International Campus of Tianjin University, Binhai New City, Fuzhou, 350207, China

b. Department of Physics, National University of Singapore, 2 Science Drive 3, 117542, Singapore

c. State Key Laboratory of High Performance Ceramics and Superfine Microstructure, Shanghai Institute of Ceramics, Chinese Academy of Sciences, Shanghai, 201899, China

d. Institute of High Performance Computing (IHPC), Agency for Science, Technology and Research (A*STAR), 1 Fusionopolis Way, #16–16 Connexis, 138632, Singapore

e. Department of Chemistry, National University of Singapore, 3 Science Drive 3, 117543, Singapore

Supplement Note 1. Computational Details.

The first-principles calculation was conducted by the VASP code.^{1,2} The RPBE functional was selected for the exchange-correlation functional.³ The ion cores were represented by projector-augmented wave (PAW) potentials.³ Plane-waves with a kinetic energy cutoff of 400 eV were used as the basis set for the valence electrons. When determining the appropriate lattice constant of bulk copper, the Monkhorst–Pack grid for k-points was set to $12 \times 12 \times 12$. The optimized lattice constant was 3.679 Å. A $3\sqrt{2} \times 3\sqrt{2}$ Cu(100) slab with three layers was chosen to model the CO–CO coupling reaction. The Brillouin zone for the slab was sampled using a $3 \times 3 \times 1$ Monkhorst-Pack grid. During the optimization, the bottom layer of the Cu(100) slab was fixed. The atomic force convergence criterion was set to 0.025 eV/Å and the total energy convergence was 1×10^{-6} eV.

Fixed potential method (FPM) was implemented by adjusting the number of electrons in the system to ensure the Fermi level in accordance with the applied electrode potential. To maintain the overall neutrality of the system, the countercharges were implicitly introduced using the linearized Poisson-Boltzmann equation, as implemented in the VASPsol code. The Debye length was set to 3 Å, corresponding to 1 M bulk electrolyte concentration. The relative permittivity of water was set to 78.4. The applied potential on the electrode with respect to the standard hydrogen electrode (SHE), U_{SHE} , and that with respect to the vacuum level, U_{abs} , can be converted through⁴

$$U_{\text{SHE}} = U_{\text{abs}} - 4.44 \quad (2)$$

where U_{SHE} and U_{abs} are commonly used in expressing the electrode potential in experiments and calculations, respectively.

In the explicit solvent calculation, the water structure was obtained by molecular dynamics (MD) simulations carried out by the ASE package,⁵ which could constrain the 18 water molecules on the copper surface and prevent them from drifting away during the MD simulations. The height of the constraint is set to 7 Å above the surface. The simulations were accelerated by machine learning interatomic potentials (MLIPs) with active learning to ensure high accuracy.⁶ The MLIP used was the moment tensor potential (MTP), as implemented in the MLIP package.⁷⁻⁹ A radial cutoff of 5 Å and lev_{max} of 20 was employed. The MD simulation consisted of an NVT simulation at 300 K for 100000 timesteps using the Nose thermostat and a cooling process from 300 K to 0 K over 30000 timesteps. The timestep was set to 1.0 fs. The explicit solvent calculation can be obtained by an optimization of the slab model. The transition states from two *CO to *OCCO were located using the dimer method and climbing-image nudged elastic band (CI-NEB) method as implemented in the VTST package.^{10,11}

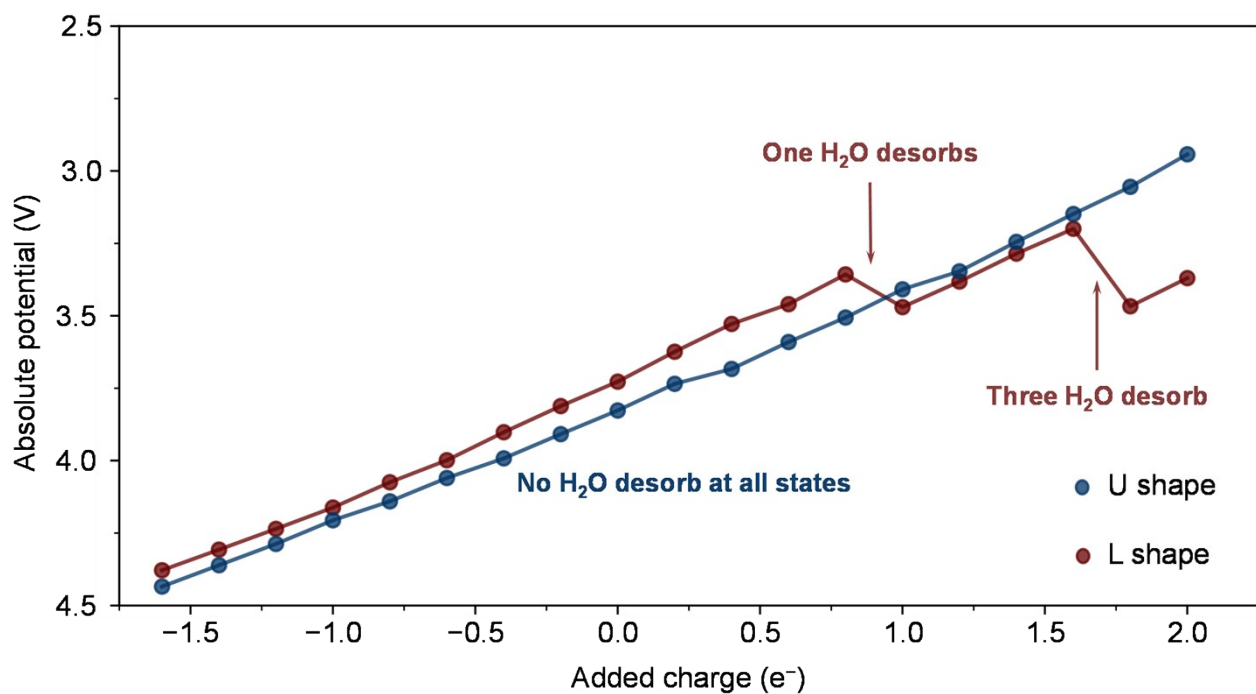


Figure S1. Relation between absolute potential (U) and added charges (q) in explicit solvent calculation on L-shape and U-shape *OCCO.

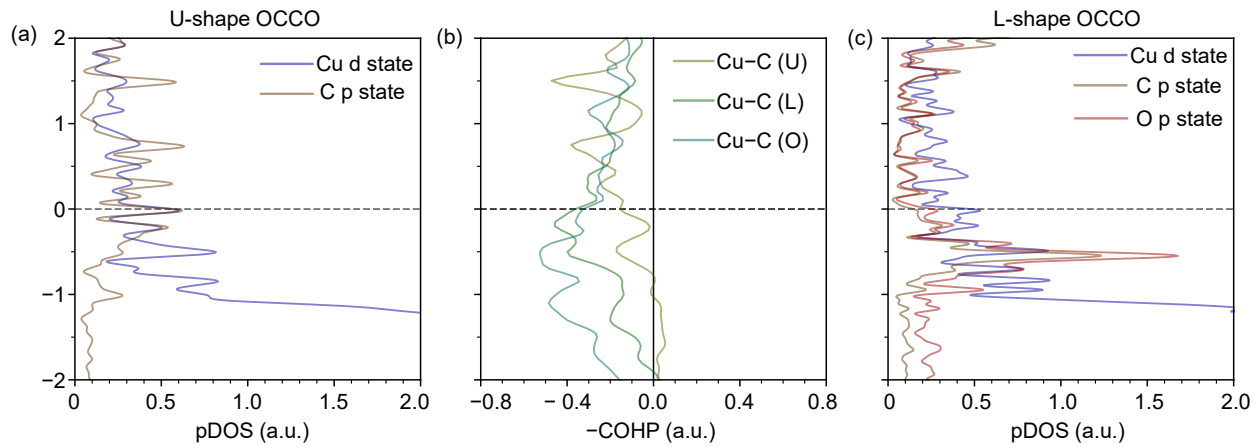


Figure S2. (a) pDOS of Cu d state and C p state in U-shape OCCO, (b) COHP analysis of Cu–C bond in U-shape *OCCO, Cu–C bond and Cu–O bond in L-shape *OCCO, (c) pDOS of Cu d state, C p state and O p state in L-shape OCCO. The Cu–C bond in U-shape and Cu–C bond and Cu–O bond in L-shape OCCO are contributed from the d state in Cu and p state in C or O.

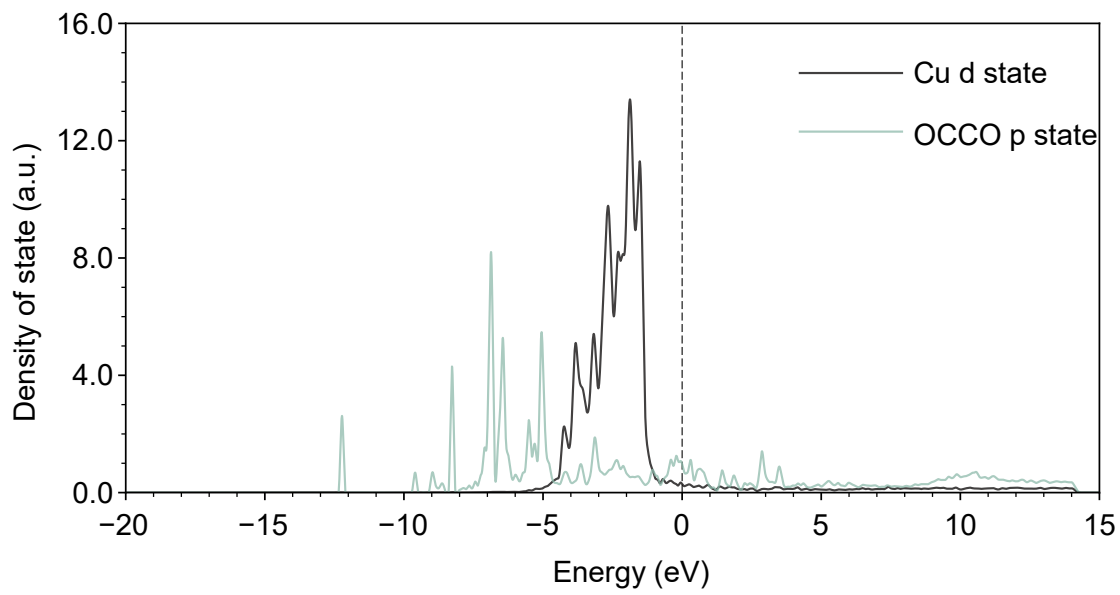


Figure S3. Density of state (DOS) of U-shape *OCCO on Cu(100) in the explicit solvent calculation. The DOS of the Cu d state is 25 times smaller than the original value for the convenience of presentation.

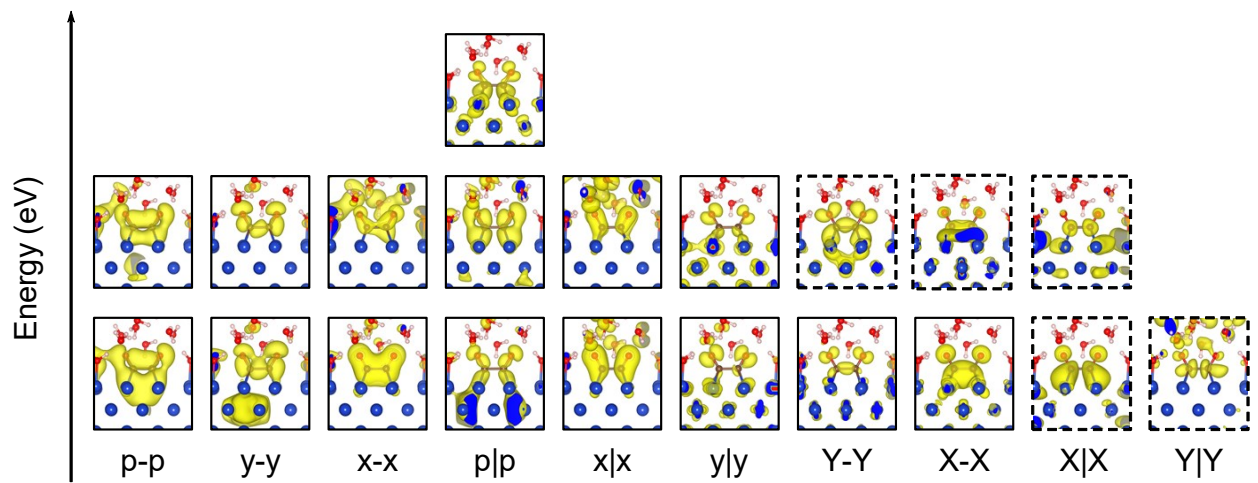


Figure S4. Partial charge densities of the OCCO orbitals with significant projections above the p orbital. The orbitals split from the same orbital of the free OCCO molecule are plot in a column. The orbitals in the column are placed from bottom to top with the order of increasing energy level. The occupied orbitals are plot with a black border line, while the orbitals which are not occupied are plot with a black dashed border line.

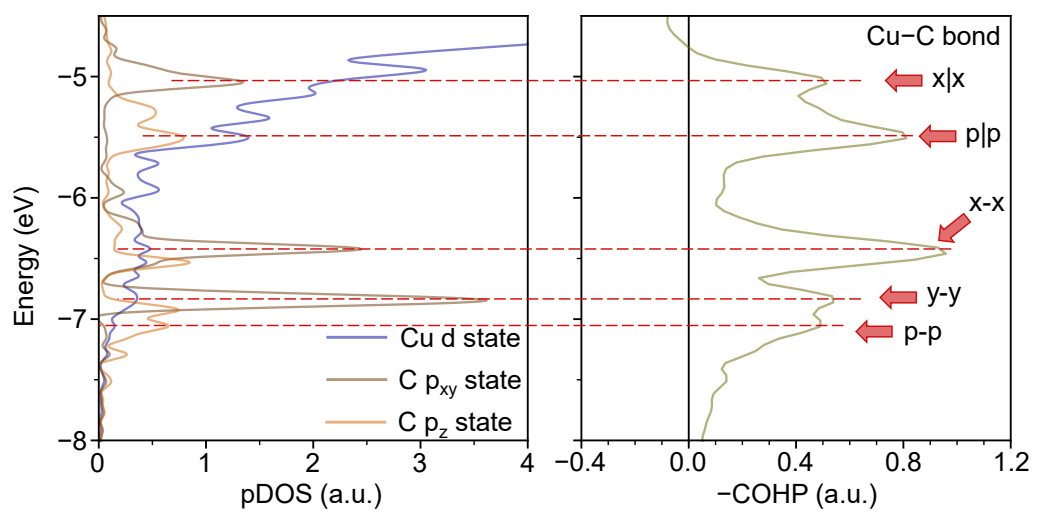


Figure S5. Partial density of state (pDOS) and COHP analysis of the Cu–C bonds in U-shape *OCCO on Cu(100) surface.⁵⁻⁸ Main MOs are labelled with red arrows.

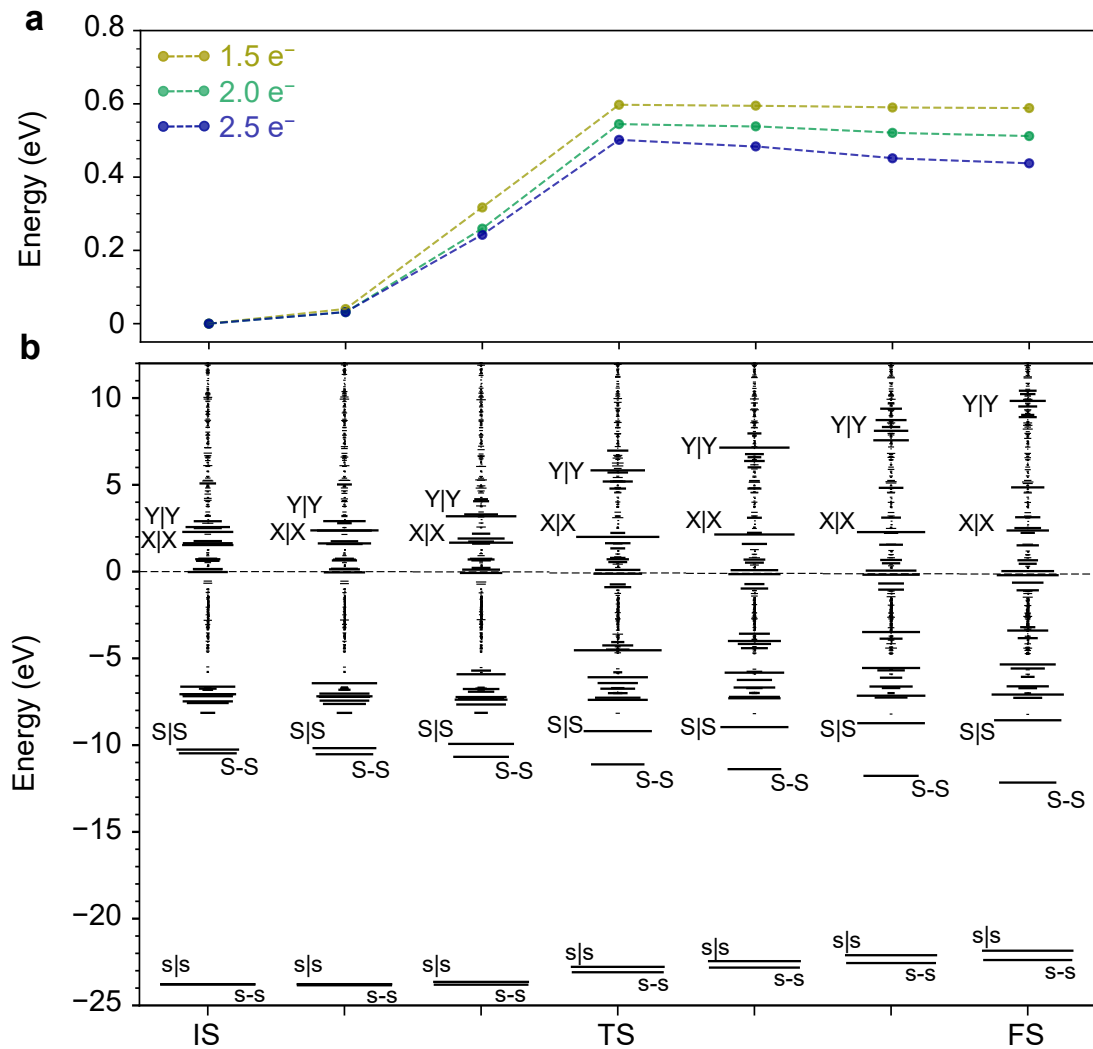


Figure S6. During the dimerization process of *OCCO on Cu (100) in implicit solvent calculation, (a) Electronic energy change under three different charge states. (b) Full range eigenvalue spectra with the significant projections on the adsorbates. The notations are labelled near the corresponding MO spectra. A wider horizontal bar in the eigenvalue spectra represents larger projection of the corresponding eigenstate on the adsorbate. The results in Figure S7a show that both the energy barrier from IS to TS and thermodynamic energy from IS to FS decrease with the increasing added electrons. The eigenvalue spectral analysis reveals similar MO splitting behavior between s-s and s|s, as well as between S-S and S|S, as observed in the free state shown in Figure S10.

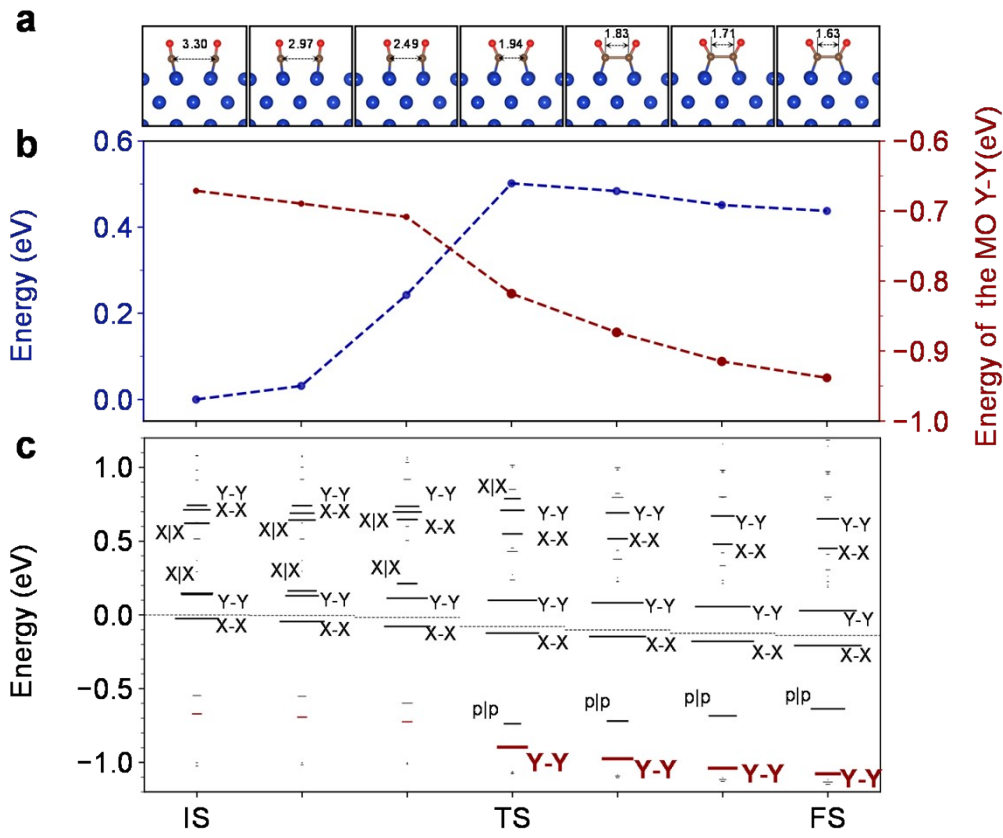


Figure S7. During CO–CO coupling reaction with 2.5 added electrons, (a) Structures of U-shape *OCCO on Cu(100) surface and distances between two C atoms in the implicit solvent calculation. (b) Electronic energy change of CO–CO coupling on Cu(100) (blue line) and energy level of the Y-Y MO (red line). Point size in the red line represents the projection value of the adsorbate. (c) Eigenvalue spectra of adsorbate during CO–CO coupling near the Fermi level. Notations are labelled near the corresponding MO spectra. A wider horizontal bar in eigenvalue spectra represents larger projection from adsorbate. During the CO–CO coupling in the implicit solvent calculation, the X-X MO remains the HOMO. Figure S12a shows that the partial charge densities of the highest occupied X-X MOs during the coupling and the X-X MO carries the C–C bonding character even in the initial state, indicating an interaction between two *CO adsorbates. Upon reaching the transition state, the Y-Y MO emerges below the X-X and p|p MOs. The evolution of the partial charge densities of the Y-Y MOs are shown in Figure S12b. The energy levels of the corresponding Y-Y MOs are highlighted in red in Figure S8c. We plotted the energy level of the highlighted Y-Y MOs in every image relative to the Fermi levels in Figure S8b, which shows a gradual decrease. We suggest that the decreasing energy level of the occupied Y-Y MO, coupled with the emergence of the Y-Y MO at the transition state, could explain the decrease of the electronic energy after the transition state in the implicit solvent calculation. Therefore, the Y-Y MO is identified as the driving force for the coupling reaction in the implicit solvent calculation.

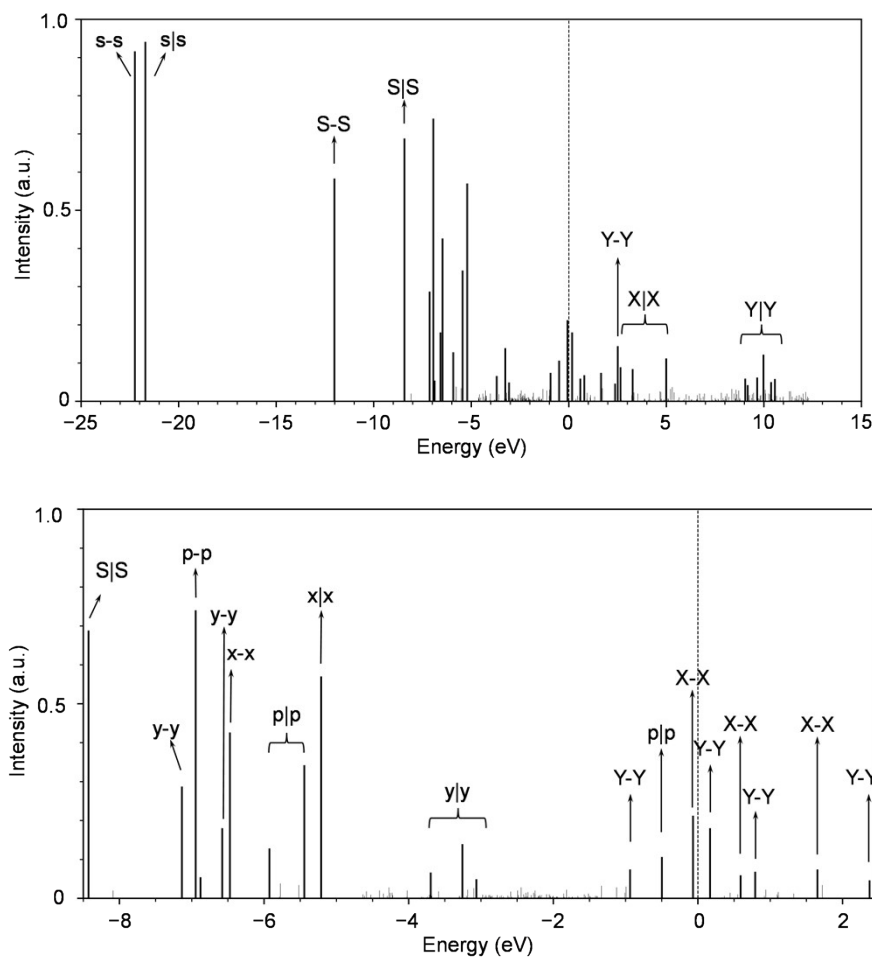


Figure S8. Eigenvalue spectra of U-shape *OCCO in the implicit solvent calculation with 2.5 charges added. Distribution and projection of MOs in the implicit solvent calculation closely resemble those in the explicit solvent calculation, especially the MOs near the Fermi level. It indicates that the explicit solvent has an insignificant impact on the MOs of the *OCCO adsorbate.

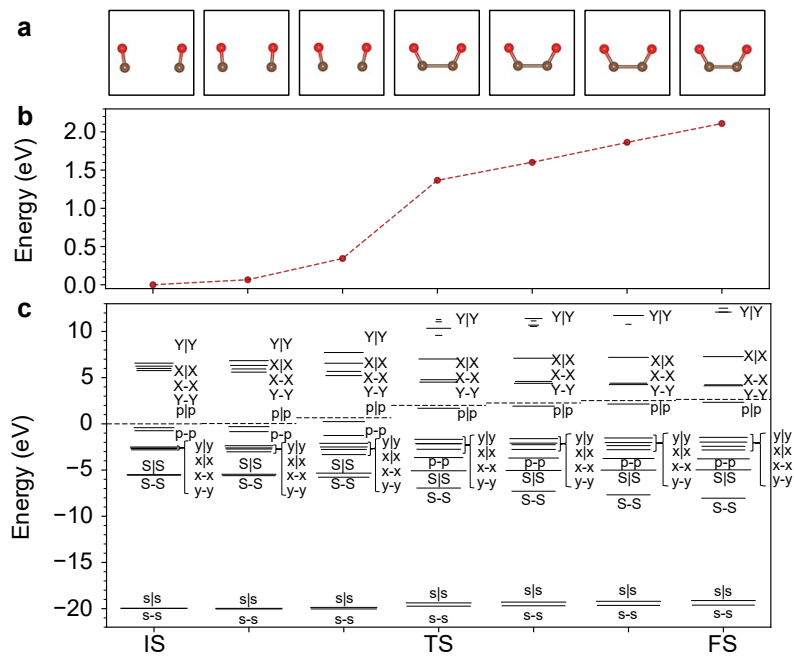


Figure S9. During the dimerization process in gas state, (a) Structures of free molecules during the process, (b) Electronic energy change and (c) Eigenvalue spectra of the molecules. Notations are labelled near the corresponding MO spectra. A wider horizontal bar in the eigenvalue spectra represents larger projection on the molecules. We analyzed the eigenvalue spectra of every image in the free state coupling reaction, as shown in Figure S10c. In the bottom of the eigenvalue spectra, the apparent splitting of σ_s orbital forms one C–C bonding and one anti-bonding MOs, that is, the s-s and s|s MOs, as well as the S-S and S|S MOs from the splitting of σ_s^* orbital. The similar phenomenon is also observed in other MOs. The splitting of the σ_p orbital is more pronounced than that of π_x and π_y orbitals. In the initial state, the two highest occupied MOs (HOMOs) are the p-p and p|p MOs, while in the final state, the energy level of the p-p MO is lower than the four orbitals originated from the π_x and π_y MOs, and p|p remains the HOMO.

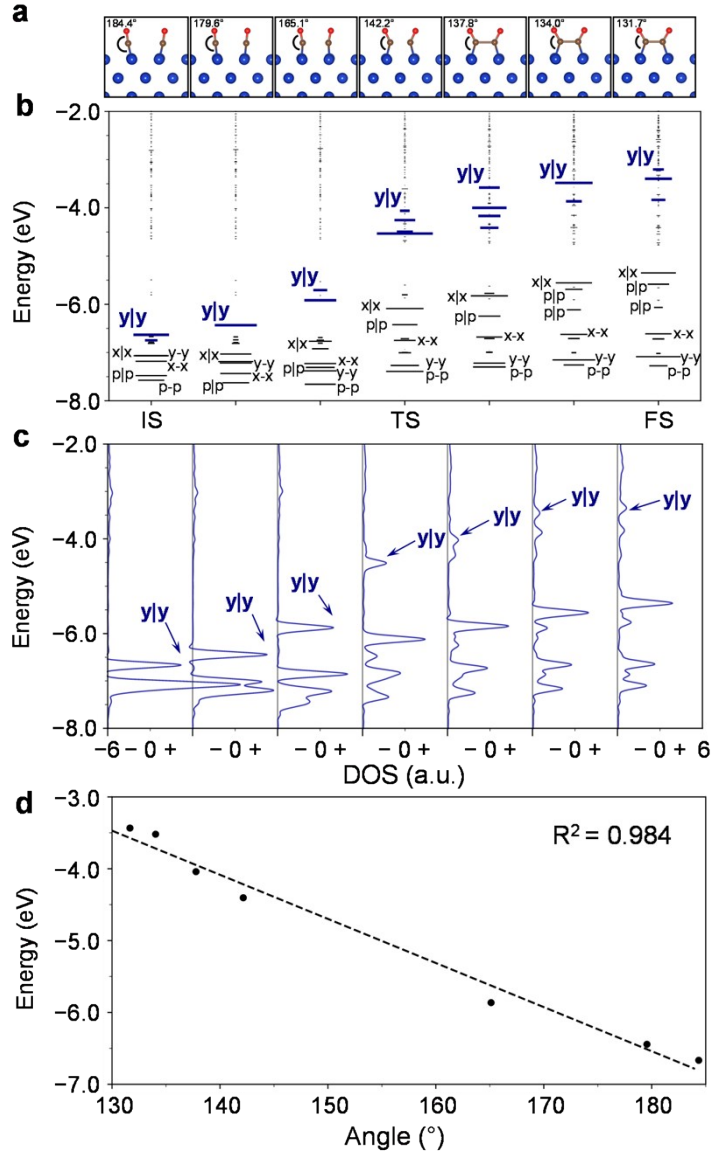


Figure S10. During CO–CO coupling, (a) Structures of adsorbates on Cu(100) surface and corresponding O–C–Cu bond angles. (b) Eigenvalue spectra of *OCCO from –8 to –2 eV. Notations are labelled near the corresponding MO spectra. (c) pDOS of p_{xy} states from C and O atoms. The arrows points to the $y|y$ MOs in every image. (d) Relationship between the state center of $y|y$ states and O–C–Cu bond angle. Structural changes during the CO–CO coupling show the O–C–Cu bond angles bend, followed by the bonding between two C atoms. The O–C–Cu bond angles in every image shows that the bond angle decreases during the reaction. If there is a *CO adsorbed on the surface, the *CO should be adsorbed vertically due to the symmetric MOs of the CO molecule about the C–O axis, as shown in Figure S13. However, the interactions exist between the two adsorbed *CO on the Cu(100) surface. The interactions make some MOs asymmetric, such as the $y|y$ MO which are depicted in Figure S14. The asymmetric MOs contribute to the bending of O–C–Cu bond angles. In Figure S11d, we plotted the relationship between the O–C–Cu bond angles and the state center of the $y|y$ MOs in pDOS. A linear relationship indicates that the decrease of the O–C–Cu bond angles during the coupling results from to the rising energy level of the $y|y$ MOs.

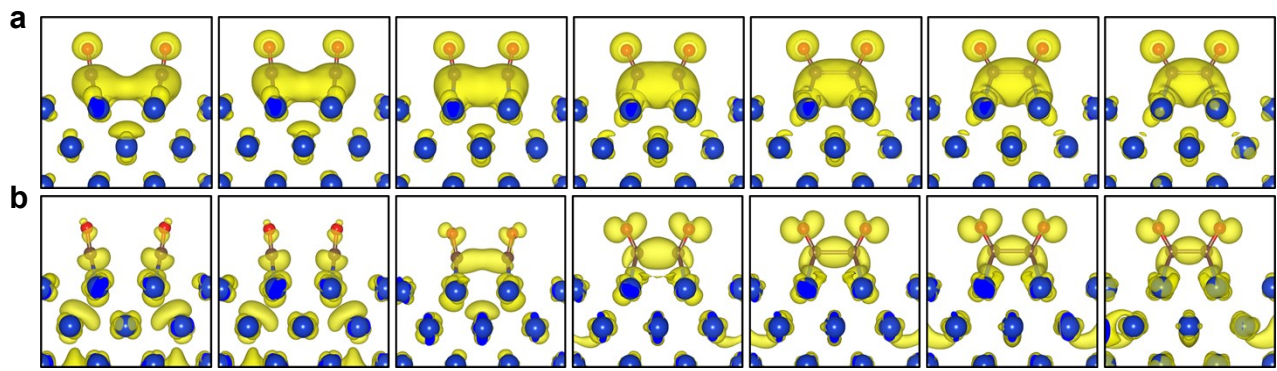


Figure S11. Partial charge densities of (a) X-X MOs, (b) Y-Y MOs, which are identified as the driving force during the dimerization reaction.

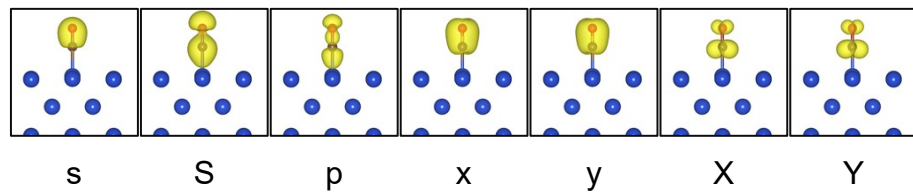


Figure S12. MOs of CO adsorbed on the Cu(100) surface.

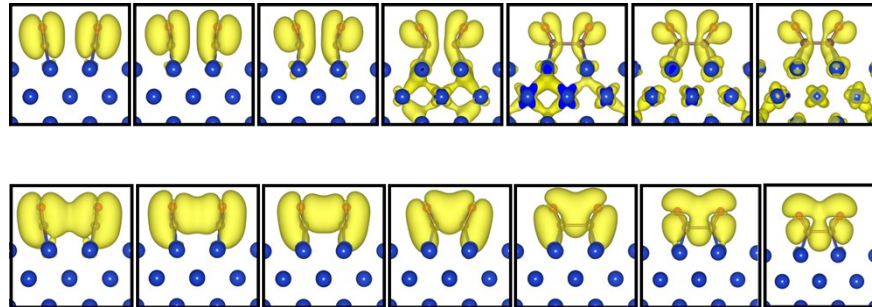


Figure S13. Partial charge densities of the y|y (upper) and y-y MOs (below) during the dimerization process.

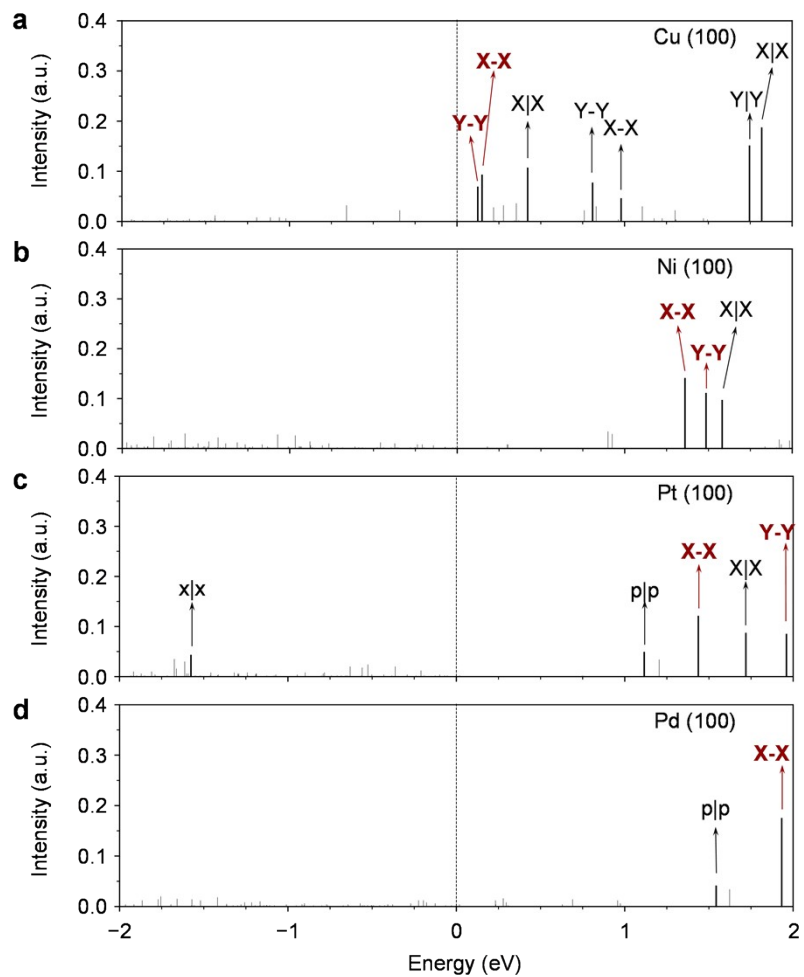


Figure S14. Eigenvalue spectra for two CO adsorbed on (a) Cu(100), (b) Ni(100), (c) Pt(100) and (d) Pd(100) surface. Main MOs near the Fermi level are plot in bold lines.

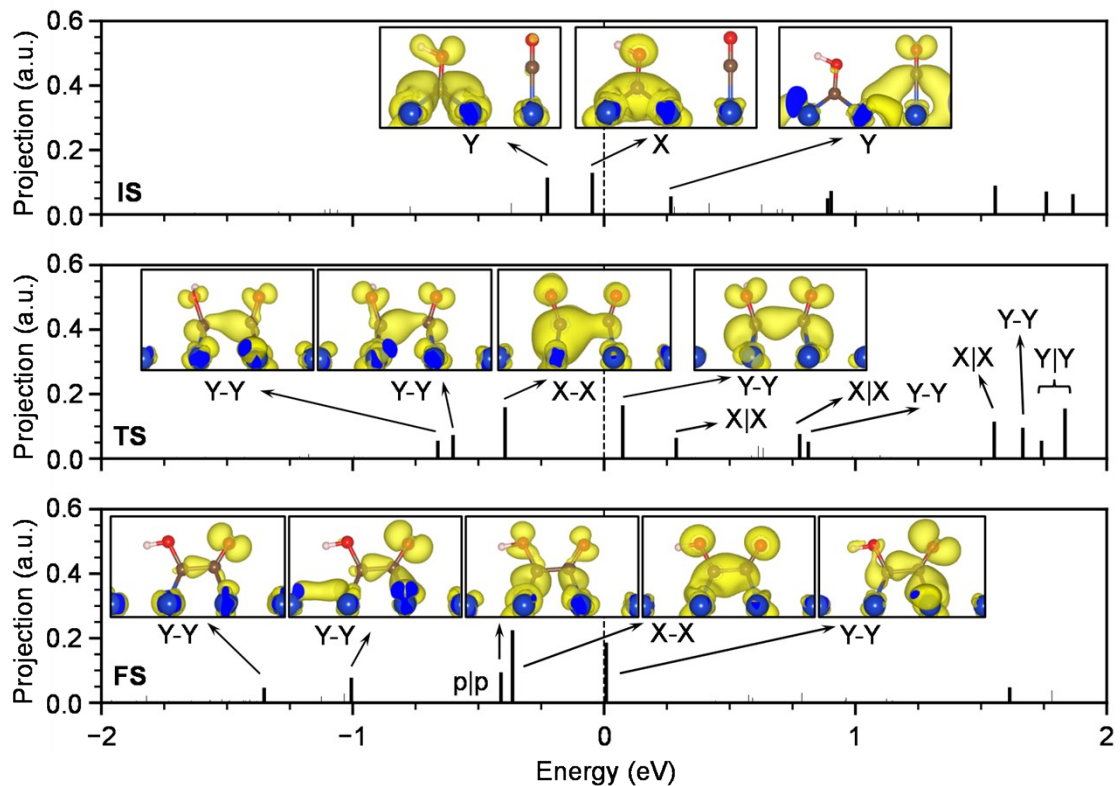


Figure S15. Eigenvalue spectra of initial state (IS), transition state (TS) and final state (FS) during the CO–COH coupling at -1.0 V (vs. SHE). The Fermi level, plotted as a dash line, is set as reference. Notations are labelled near the corresponding MOs. Visual representations of partial charge density for frontier MOs are plotted as insets in IS, TS and FS, respectively.

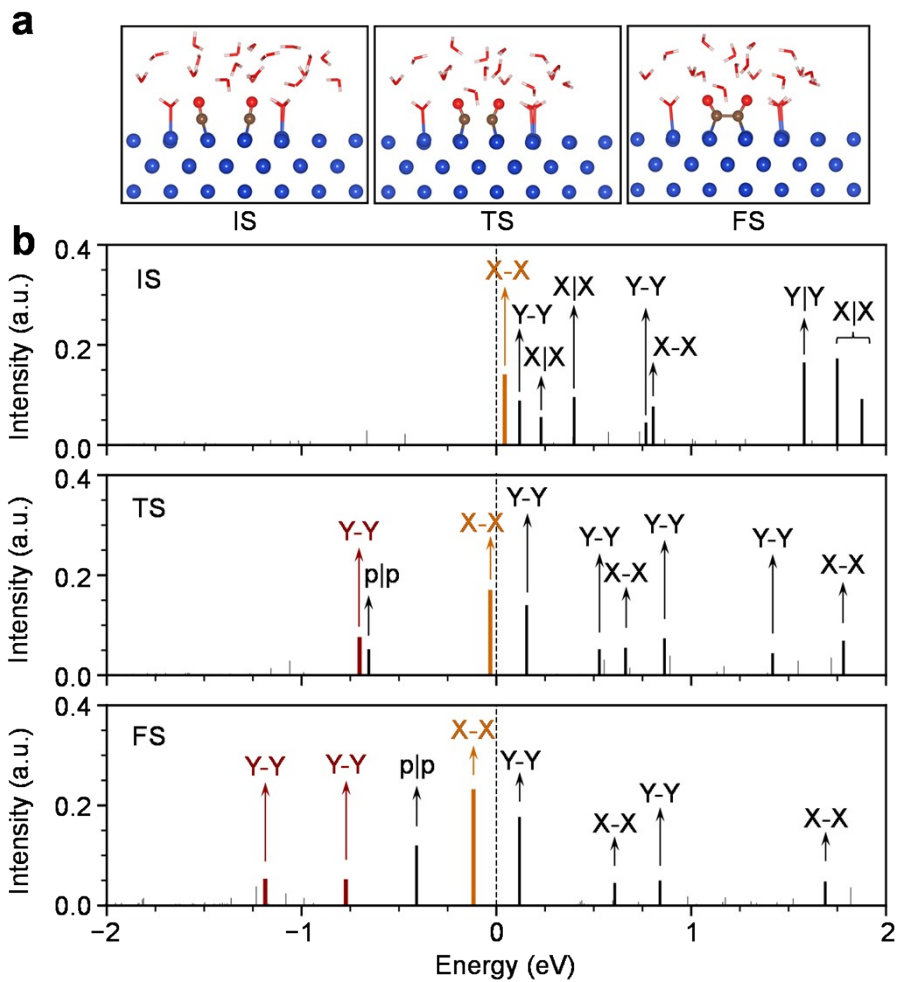


Figure S16. (a) Atomic structures of initial state (IS), transition state (TS) and final state (FS) during the CO–CO coupling process with a different water structure from the that in figure 4 in the manuscript. (b) Eigenvalue spectra of IS, TS and FS under the new water structure at $U = -1$ V (vs. SHE). The Fermi level, plotted as a dash line, is set as reference. Notations are labelled near the corresponding MOs. The results obtained from this explicit water structure are similar to those presented in the manuscript. This consistency suggests that the C–C coupling mechanism is not sensitively dependent on detailed explicit water structure. This insensitivity is understandable by the fact that the energy levels of the water molecules do not significantly impact the distribution of the frontier MOs (e.g., X-X and Y-Y).

Table S1. The frequencies of the transition states during the CO-CO coupling reaction at 0, −0.5 and −1.0 V, respectively.

Frequency (cm ⁻¹) @ 0 V	Frequency (cm ⁻¹) @ -0.5 V	Frequency (cm ⁻¹) @ -1.0 V
1611.532	1614.155	1608.737
1520.192	1532.720	1537.224
568.611	546.530	527.179
294.172	290.472	308.672
268.016	272.941	256.960
243.843	248.140	251.358
227.224	229.681	232.664
216.493	219.961	227.107
126.829	129.557	133.593
114.141	113.987	113.716
99.852	100.530	95.048
245.145 (imaginary frequency)	319.224 (imaginary frequency)	333.616 (imaginary frequency)

POSCAR structure files in the calculations

L-shape OCCO on Cu(100) surface without added electrons

1.00000000000000

11.038299999999996 0.000000000000000 0.000000000000000

0.000000000000000 11.038299999999996 0.000000000000000

0.000000000000000 0.000000000000000 22.000000000000000

Cu H O C

54 36 20 2

Selective dynamics

Direct

0.1666700000000034 0.000000000000000 0.000000000000000 F F F
0.500000000000000 0.000000000000000 0.000000000000000 F F F
0.8333299999999966 0.000000000000000 0.000000000000000 F F F
0.000000000000000 0.1666700000000034 0.000000000000000 F F F
0.3333299999999966 0.1666700000000034 0.000000000000000 F F F
0.6666700000000034 0.1666700000000034 0.000000000000000 F F F
0.1666700000000034 0.3333299999999966 0.000000000000000 F F F
0.500000000000000 0.3333299999999966 0.000000000000000 F F F
0.8333299999999966 0.3333299999999966 0.000000000000000 F F F
0.000000000000000 0.500000000000000 0.000000000000000 F F F
0.3333299999999966 0.500000000000000 0.000000000000000 F F F
0.6666700000000034 0.500000000000000 0.000000000000000 F F F
0.1666700000000034 0.6666700000000034 0.000000000000000 F F F
0.500000000000000 0.6666700000000034 0.000000000000000 F F F
0.8333299999999966 0.6666700000000034 0.000000000000000 F F F
0.000000000000000 0.8333299999999966 0.000000000000000 F F F
0.3333299999999966 0.8333299999999966 0.000000000000000 F F F
0.6666700000000034 0.8333299999999966 0.000000000000000 F F F
0.0029062248583445 0.9991775791848970 0.0817596020392941 T T T
0.3334072893673179 0.0024609229956911 0.0836766726955891 T T T
0.6664805417113779 0.9982932278200309 0.0827931227978691 T T T
0.1690104394506803 0.1646843240683411 0.0827004669609944 T T T

0.5002597185408203	0.1668556903761081	0.0802665576401986	T	T	T
0.8311220045726554	0.1684981582788568	0.0828781919341210	T	T	T
0.9973302177615263	0.3335814915544350	0.0813297216834692	T	T	T
0.3330327947846305	0.3333345233604177	0.0806549947056844	T	T	T
0.6668103686601897	0.3312580874741533	0.0838415394568507	T	T	T
0.1661391429426473	0.5006284794883781	0.0797432020850540	T	T	T
0.4995701753819907	0.4967352402671729	0.0809651454758819	T	T	T
0.8335035832093665	0.4978968655879120	0.0815483595101250	T	T	T
0.0002490447282039	0.6676305310279785	0.0800053065975007	T	T	T
0.3326770096217756	0.6669904836438895	0.0796435376546353	T	T	T
0.6668057253256852	0.6682790188278406	0.0814990690959660	T	T	T
0.1665044023087445	0.8358282823668086	0.0816561175395933	T	T	T
0.5025624764494244	0.8354364071199976	0.0825788838877701	T	T	T
0.8308507842217580	0.8326171238199105	0.0818421550826932	T	T	T
0.1668844209032746	0.9977720694988290	0.1702426754002777	T	T	T
0.4977821140206195	0.9955576970444694	0.1652124886530437	T	T	T
0.8384352616789165	0.9972357247143850	0.1608720339819764	T	T	T
0.0015329289208720	0.1664199615329577	0.1605155932868641	T	T	T
0.3287122013195532	0.1741750352544051	0.1661403685117289	T	T	T
0.6724876732311187	0.1642941690476836	0.1651410653938858	T	T	T
0.1621600616273783	0.3377865018535187	0.1605740722844295	T	T	T
0.4967858098454107	0.3413412915342338	0.1668580976783790	T	T	T
0.8368167973744159	0.3385656501173921	0.1700094942606750	T	T	T
0.0045351605099922	0.5058431498732818	0.1615925225014277	T	T	T
0.3270459898350104	0.5037298157122039	0.1612793152234198	T	T	T
0.6657039134143939	0.5029058309455783	0.1608382981894608	T	T	T
0.1661112460464615	0.6683655572322784	0.1621662910241663	T	T	T
0.4962805822695652	0.6619396497146491	0.1602698116541454	T	T	T
0.8370575937847917	0.6633677582267922	0.1619281372928853	T	T	T
0.9980953806800376	0.8286784276228160	0.1622656864287427	T	T	T
0.3346722973230450	0.8288205062826388	0.1601793959301674	T	T	T
0.6697490331086310	0.8256931893317083	0.1701507737324277	T	T	T

0.0498402673527112	0.2281821527483471	0.4458971414254672	T	T	T
0.9878773147498885	0.4990795809797033	0.3741567725376451	T	T	T
0.2954713393798976	0.4796769249456894	0.5117014558549400	T	T	T
0.0938784596734534	0.4942280098163641	0.3281549131254317	T	T	T
0.1251791526552605	0.4558694912340482	0.5767987484785533	T	T	T
0.7204649337541729	0.6028168404458114	0.4984754164896700	T	T	T
0.7353788736417022	0.1865885488373681	0.4699434897453243	T	T	T
0.0908012296742659	0.3931599715561246	0.5155402958383739	T	T	T
0.7199995720961317	0.3117102761779853	0.5037564235066785	T	T	T
0.1616701813744506	0.8181098946691343	0.5035388307839211	T	T	T
0.8745086627918356	0.9079648717646542	0.3528119572836546	T	T	T
0.2514582727103923	0.9403449385708873	0.2858727151189338	T	T	T
0.9280961649783278	0.2680269615492977	0.4773827547140084	T	T	T
0.3968384277158896	0.4533046330085033	0.4644984024502445	T	T	T
0.7601967002210492	0.7362689549257911	0.4916165155581731	T	T	T
0.0366763225156986	0.7638567699333080	0.5182113386536915	T	T	T
0.1582721918558196	0.0437920257708591	0.2995627749166598	T	T	T
0.8355143212183139	0.0348894621764334	0.3298138558438622	T	T	T
0.3674367848894425	0.0337730663118144	0.4812358667077193	T	T	T
0.6576631892220991	0.5408371432106680	0.3503349805801148	T	T	T
0.4888161161489524	0.8985564274847424	0.5409415114466559	T	T	T
0.2633042026120236	0.1058659877114173	0.5123035247541370	T	T	T
0.6856343792979912	0.6493935065259798	0.3928789165086792	T	T	T
0.4621455489733263	0.8617456179365548	0.3019390221229446	T	T	T
0.1870350297760951	0.2227181716004812	0.3602998819212870	T	T	T
0.6981729345448100	0.8788850241179899	0.2935985225506103	T	T	T
0.6493401341795015	0.7461162320189370	0.2939608973562137	T	T	T
0.9153394105142248	0.3935258110807295	0.2862480505864743	T	T	T
0.7077608565912065	0.3369780834888858	0.3974550221273201	T	T	T
0.7412839781662018	0.0006962158405731	0.4256628435609254	T	T	T
0.4732617749967549	0.8411922788844765	0.4769956036357205	T	T	T
0.3619932924691763	0.7833008175554762	0.3318745465791429	T	T	T

0.2082523521306217	0.1238979246532673	0.4092404398888316	T	T	T
0.6374464411247139	0.9917837836207370	0.4745571633049233	T	T	T
0.7855808304778504	0.3397358338396659	0.2947755874160403	T	T	T
0.5993228430857597	0.3275447180291170	0.3527476789842333	T	T	T
0.0163703955868359	0.2611625299443873	0.4839323098271165	T	T	T
0.3821805716926091	0.4943860683724102	0.5029789867824768	T	T	T
0.0061505733768390	0.5029412425668295	0.3308363319143970	T	T	T
0.7612155333318342	0.6583972575286193	0.4707495323215374	T	T	T
0.1318536063235434	0.4654057179896835	0.5328835350599145	T	T	T
0.7588698709664515	0.2740726555677808	0.4686921624113679	T	T	T
0.0753298258094617	0.8308470933295440	0.4968774992643423	T	T	T
0.1743768839718258	0.9766287514063269	0.2713508831095429	T	T	T
0.8038160350261212	0.9599404794459397	0.3471499074508818	T	T	T
0.4875553699067025	0.9180875805318078	0.4976721523929802	T	T	T
0.3100978291508373	0.1012431572830712	0.4748146666168825	T	T	T
0.6472284095127435	0.6291941718462272	0.3536476218684631	T	T	T
0.3826933238934032	0.8668554497782726	0.3218595209947789	T	T	T
0.1475185704302147	0.1532339001631802	0.3793772646942015	T	T	T
0.6413533018140800	0.8243919005092716	0.2719079469396191	T	T	T
0.7171455311588658	0.0287705391479013	0.4664739644755357	T	T	T
0.8584002402374584	0.3334471907399393	0.2685645165391208	T	T	T
0.6776422045268736	0.3669675180901986	0.3575311295372556	T	T	T
0.3443682949055955	0.3141986514093464	0.3141687491460267	T	T	T
0.5500585409022422	0.1181002996006187	0.2327862352473596	T	T	T
0.4024954466691967	0.2594637024319533	0.2766709396803642	T	T	T
0.4613698404018660	0.2083287466252798	0.2305910078278698	T	T	T

U-shape OCCO on Cu(100) surface without added electrons

1.000000000000000

11.038299999999996 0.000000000000000 0.000000000000000

0.000000000000000 11.038299999999996 0.000000000000000

0.0000000000000000 0.0000000000000000 22.0000000000000000

Cu H O C

54 36 20 2

Selective dynamics

Direct

0.1666700000000034	0.0000000000000000	0.0000000000000000	F F F
0.5000000000000000	0.0000000000000000	0.0000000000000000	F F F
0.8333299999999966	0.0000000000000000	0.0000000000000000	F F F
0.0000000000000000	0.1666700000000034	0.0000000000000000	F F F
0.3333299999999966	0.1666700000000034	0.0000000000000000	F F F
0.6666700000000034	0.1666700000000034	0.0000000000000000	F F F
0.1666700000000034	0.3333299999999966	0.0000000000000000	F F F
0.5000000000000000	0.3333299999999966	0.0000000000000000	F F F
0.8333299999999966	0.3333299999999966	0.0000000000000000	F F F
0.0000000000000000	0.5000000000000000	0.0000000000000000	F F F
0.3333299999999966	0.5000000000000000	0.0000000000000000	F F F
0.6666700000000034	0.5000000000000000	0.0000000000000000	F F F
0.1666700000000034	0.6666700000000034	0.0000000000000000	F F F
0.5000000000000000	0.6666700000000034	0.0000000000000000	F F F
0.8333299999999966	0.6666700000000034	0.0000000000000000	F F F
0.0000000000000000	0.8333299999999966	0.0000000000000000	F F F
0.3333299999999966	0.8333299999999966	0.0000000000000000	F F F
0.6666700000000034	0.8333299999999966	0.0000000000000000	F F F
0.0004517448294134	0.0013001967296697	0.0801195368612696	T T T
0.3347596303792559	0.0022990000180856	0.0816243202433224	T T T
0.6654644359361320	0.0000316238185820	0.0810843712636394	T T T
0.1683911218629478	0.1691214041196598	0.0818732107551894	T T T
0.4995492738452514	0.1643424076002089	0.0818229175038235	T T T
0.8346016652559121	0.1695154883102263	0.0816919816956551	T T T
0.0001653509763614	0.3335764992716115	0.0827290013479659	T T T
0.3329611704989420	0.3328767118011943	0.0796130132859917	T T T
0.6662185834184778	0.3358370109664002	0.0841503286241954	T T T

0.1666627914955345	0.5011271132624912	0.0818859781533640	T	T	T
0.4992608633185830	0.4972793972821261	0.0832312255096547	T	T	T
0.8305173080605811	0.4977844673001399	0.0831063925244941	T	T	T
0.0026372722013343	0.6674000931845787	0.0811523668992189	T	T	T
0.3306175165860560	0.6640464723302617	0.0817803411779701	T	T	T
0.6664508233769199	0.6639691710095319	0.0811122190274920	T	T	T
0.1657284888171031	0.8321601489453569	0.0810843348761078	T	T	T
0.5009237274261290	0.8355747492242952	0.0810154705867122	T	T	T
0.8337807344875990	0.8337037267718687	0.0796860333989553	T	T	T
0.1658865485014580	0.9988214020882793	0.1613526062789111	T	T	T
0.5032351740654732	0.9942514343305965	0.1686198925075443	T	T	T
0.8344181194228405	0.9993870672071696	0.1615871720589157	T	T	T
0.0041209858278244	0.1631896683013354	0.1619371186280659	T	T	T
0.3304753539535339	0.1648572557819623	0.1657838174860780	T	T	T
0.6696534253749363	0.1645487369485114	0.1598437189998199	T	T	T
0.1648541017824523	0.3377830626424567	0.1674532491560659	T	T	T
0.4972314962243106	0.3242015507431758	0.1662443004618896	T	T	T
0.8367010616334608	0.3318578119051316	0.1699726203958441	T	T	T
0.9984712242312225	0.5036826042591667	0.1604698680014570	T	T	T
0.3316133862837964	0.4974501312352749	0.1650107154509779	T	T	T
0.6638233293685493	0.5031725639102852	0.1678909643710066	T	T	T
0.1637158478677383	0.6730089579167748	0.1689116899734031	T	T	T
0.4961445946807355	0.6709599925955571	0.1597121328479360	T	T	T
0.8371507650522751	0.6702768132276238	0.1606928471143166	T	T	T
0.9967623447823535	0.8379492874485990	0.1619394878453582	T	T	T
0.3321738736098577	0.8350783302298249	0.1593542089982654	T	T	T
0.6719297230811243	0.8310259234564775	0.1604821834538879	T	T	T
0.4554592545927506	0.9391251878706519	0.2862645077829792	T	T	T
0.9868438195695292	0.4593122315228629	0.3770144317744020	T	T	T
0.3459544502014087	0.8365847336845269	0.4767029906772823	T	T	T
0.9436835463726508	0.5774693083332973	0.3451260592283282	T	T	T
0.9999148775805444	0.1245800463837017	0.4172993078301325	T	T	T

0.9317710702659742	0.7944730135798679	0.3220579629771527	T	T	T
0.4462439388484346	0.7530869543692005	0.3382238526961779	T	T	T
0.0792025319528564	0.2390704036874776	0.4291110639404347	T	T	T
0.3184333228360466	0.7665783035519788	0.3089227305967571	T	T	T
0.6992789361591663	0.7267397573240700	0.5331638435352520	T	T	T
0.4550871559365423	0.1396905641597559	0.4786417305247503	T	T	T
0.7308429084821945	0.4245025098038587	0.4668453853171317	T	T	T
0.4687114678490664	0.0825330729379905	0.2779500813076679	T	T	T
0.3328457217844435	0.8624187007613010	0.4070824005625131	T	T	T
0.0139344188569725	0.7696808157631253	0.3794443963110760	T	T	T
0.6088053635223574	0.8216107041178069	0.5578598178285112	T	T	T
0.6080749215129800	0.3682199279026612	0.4858390518921233	T	T	T
0.3496060939148499	0.0482193716870218	0.4666631530914229	T	T	T
0.2537343356874691	0.4479079102075328	0.4770579338431756	T	T	T
0.2574556106866615	0.3292350256967168	0.3808511673015985	T	T	T
0.1160933965549621	0.6962788891670857	0.2918080965706798	T	T	T
0.3243533986708272	0.4997796639337408	0.5321727956555132	T	T	T
0.2877875875763125	0.2471443180414756	0.4378992374178283	T	T	T
0.6816728005721771	0.6056528786743742	0.2807317530206824	T	T	T
0.1424988415312563	0.8437516775821374	0.4523886997225846	T	T	T
0.6880189508385722	0.8926353810880042	0.4608320519945414	T	T	T
0.6511706706391535	0.9925955347428793	0.4147058203656865	T	T	T
0.7659368683387286	0.3102093509546191	0.2881668003822577	T	T	T
0.5468477103795724	0.3028618494947595	0.3267987435259599	T	T	T
0.9480004520865708	0.2043686640197883	0.5170183566232605	T	T	T
0.2063026839430488	0.5850187420457297	0.2796756887556383	T	T	T
0.6235390675313671	0.4762351273937676	0.2906428649459100	T	T	T
0.0088534077394320	0.8755443852850451	0.4701178220667662	T	T	T
0.8409395351346293	0.1809941486776359	0.5613647080642692	T	T	T
0.8847573355403169	0.3850461899373736	0.2911808962733274	T	T	T
0.6288099265735527	0.3646947748472474	0.3782000838795029	T	T	T
0.5048116052697037	0.0027550195767485	0.2663809442562624	T	T	T

0.3048083224206084	0.8894086741976868	0.4477272082070447	T	T	T
0.9232150958353760	0.4910255502634258	0.3508287828009845	T	T	T
0.9907493585666405	0.7375291529975384	0.3385329621667195	T	T	T
0.9973810426572564	0.2049157820473123	0.4355838697015239	T	T	T
0.3823745312442339	0.8123031984758484	0.3304334500600771	T	T	T
0.6336299646419322	0.7803794525164301	0.5206892886556675	T	T	T
0.6457823236640760	0.4194960436361821	0.4551056305330783	T	T	T
0.3671259423463992	0.1324209518463969	0.4793455424646451	T	T	T
0.1904774801353958	0.6717561521464707	0.2691621671289375	T	T	T
0.2582518435885309	0.5185135353081850	0.5043868335644104	T	T	T
0.2326925700446660	0.3118310930577604	0.4226775142736838	T	T	T
0.6255366370216174	0.5477358158783288	0.2626228143077564	T	T	T
0.0587540470607347	0.8116079650320119	0.4526165747143089	T	T	T
0.7209849278292981	0.9473812317150274	0.4294612373771614	T	T	T
0.9247803223617044	0.2084081113901233	0.5603781971716286	T	T	T
0.8457789674021644	0.3177361674325944	0.2682472314669226	T	T	T
0.6242939116313149	0.3446974774226780	0.3341866247283758	T	T	T
0.2548494581320410	0.4332049870785283	0.2875238914191158	T	T	T
0.4125906514300732	0.2296247262626808	0.2869857052570925	T	T	T
0.2891538886773838	0.3861427336010262	0.2376953046055962	T	T	T
0.3746606708175521	0.2754991415457174	0.2370728528695501	T	T	T

Initial state in the CO–CO coupling on Cu(100) surface

1.00000000000000

11.038299999999996 0.000000000000000 0.000000000000000

0.000000000000000 11.038299999999996 0.000000000000000

0.000000000000000 0.000000000000000 22.000000000000000

Cu H O C

54 36 20 2

Selective dynamics

Direct

0.1666700000000034 0.000000000000000 0.000000000000000 F F F

0.5000000000000000	0.0000000000000000	0.0000000000000000	F F F
0.8333299999999966	0.0000000000000000	0.0000000000000000	F F F
0.0000000000000000	0.1666700000000034	0.0000000000000000	F F F
0.3333299999999966	0.1666700000000034	0.0000000000000000	F F F
0.6666700000000034	0.1666700000000034	0.0000000000000000	F F F
0.1666700000000034	0.3333299999999966	0.0000000000000000	F F F
0.5000000000000000	0.3333299999999966	0.0000000000000000	F F F
0.8333299999999966	0.3333299999999966	0.0000000000000000	F F F
0.0000000000000000	0.5000000000000000	0.0000000000000000	F F F
0.3333299999999966	0.5000000000000000	0.0000000000000000	F F F
0.6666700000000034	0.5000000000000000	0.0000000000000000	F F F
0.1666700000000034	0.6666700000000034	0.0000000000000000	F F F
0.5000000000000000	0.6666700000000034	0.0000000000000000	F F F
0.8333299999999966	0.6666700000000034	0.0000000000000000	F F F
0.0000000000000000	0.8333299999999966	0.0000000000000000	F F F
0.3333299999999966	0.8333299999999966	0.0000000000000000	F F F
0.6666700000000034	0.8333299999999966	0.0000000000000000	F F F
-0.0002435340293386	0.0008001926148923	0.0804435763708100	T T T
0.3354056827426601	0.0007957115791210	0.0821268191771452	T T T
0.6660428884258364	-0.0012903049693991	0.0816982570031207	T T T
0.1685568532897016	0.1682686111216965	0.0819827474595102	T T T
0.5012568369985593	0.1631239829999230	0.0800298936672063	T T T
0.8342509175534600	0.1688866583493162	0.0820348159551777	T T T
-0.0013472351636388	0.3331480400910058	0.0824255258093615	T T T
0.3328500425488563	0.3324090332717231	0.0789348098278156	T T T
0.6666395959429009	0.3354332993205877	0.0845079104931126	T T T
0.1649762547524346	0.5009941754236331	0.0788153890621002	T T T
0.4983173489704725	0.4959999738481057	0.0837767849679004	T T T
0.8296519490530397	0.4980532510591236	0.0834316783540823	T T T
0.0000765426273623	0.6682598299689956	0.0806374940717860	T T T
0.3313045253569486	0.6648864547554776	0.0812081455486958	T T T
0.6656613787989406	0.6636373321412193	0.0820694692813735	T T T

0.1652398560418594	0.8345187758297460	0.0804812350266378	T	T	T
0.5007353279777231	0.8335666666642576	0.0813914740524732	T	T	T
0.8332849140549494	0.8338815464804360	0.0804585847479216	T	T	T
0.1658795015975062	0.9988371861454659	0.1626293051243213	T	T	T
0.5012440081716178	0.9933766642439007	0.1681361480145856	T	T	T
0.8345773623572628	-0.0002257887955991	0.1622772438348025	T	T	T
0.0027034334307262	0.1622412005752994	0.1626830610240148	T	T	T
0.3295141459691969	0.1621712797992535	0.1656347892848408	T	T	T
0.6693650985193996	0.1642662518011555	0.1606500750558741	T	T	T
0.1625438948226421	0.3331777091941946	0.1649716965928459	T	T	T
0.4973220761739162	0.3259304812749784	0.1655061352556120	T	T	T
0.8370011279302398	0.3314803452087987	0.1708724263367290	T	T	T
-0.0001017845128638	0.5040067274569455	0.1603624734624241	T	T	T
0.3287169601457748	0.5000158358710032	0.1648900126256275	T	T	T
0.6621544689425253	0.5021107465730594	0.1691428264902214	T	T	T
0.1633799787216758	0.6726192092549258	0.1635775577125760	T	T	T
0.4932796677197488	0.6687769077509625	0.1609024633185771	T	T	T
0.8374626367658948	0.6693811073966766	0.1612716800491067	T	T	T
0.9981635605373713	0.8367861560448991	0.1626998974989880	T	T	T
0.3293470722747361	0.8336503672030213	0.1607008614576922	T	T	T
0.6715680733709792	0.8306074574901463	0.1611651014171162	T	T	T
0.4733623370589116	0.9123473438113017	0.2921387526506701	T	T	T
0.9809144029391296	0.4846909485611414	0.3813484977306367	T	T	T
0.3141008334623382	0.8582767269434729	0.4895644447005750	T	T	T
0.9263823468915932	0.6011015652464097	0.3521133554461363	T	T	T
0.0307101500694224	0.1218526733409752	0.3967904310543415	T	T	T
0.9017413607426656	0.8262794055690688	0.3309962253528121	T	T	T
0.4292665833061964	0.7646961962046087	0.3579936990835526	T	T	T
0.0947809802576735	0.2409709807554981	0.4173934689449953	T	T	T
0.3042157388779925	0.7914027630450098	0.3271008813343754	T	T	T
0.6661901288404141	0.7217074750853558	0.5180988688611540	T	T	T
0.4523031930918738	0.1488478661622923	0.4865776656250156	T	T	T

0.7180606665847316 0.4568607719174069 0.4816092637597173 T T T
0.5734216190413663 0.0137552972503445 0.2900230436471962 T T T
0.3147464371810270 0.8841082981028703 0.4196189652124717 T T T
-0.0233271941101717 0.8057039618252940 0.3912988053188566 T T T
0.5726485648674884 0.8033522076970017 0.5505188194482453 T T T
0.6068076714613255 0.3775639327518341 0.4977098146715214 T T T
0.3392231812264572 0.0648073150862710 0.4780093556859220 T T T
0.2261283508602287 0.4660217544998598 0.4802789263216770 T T T
0.2793230398455535 0.3451028135388319 0.3932104938843958 T T T
0.0991928370592921 0.7416237309356656 0.3127547288812632 T T T
0.2918473797165648 0.5659284702344201 0.5173210934249557 T T T
0.2899592594317332 0.2617563409931314 0.4508946240487468 T T T
0.6853530164942111 0.6081919787536686 0.2830373983327017 T T T
0.1135202274532309 0.8767520058695044 0.4621981419720808 T T T
0.6624852542822534 0.9159831839497866 0.4679861706187526 T T T
0.6418770587078244 -0.0003429166385468 0.4123145658693246 T T T
0.7722945976388482 0.3164397148579680 0.2928439784101280 T T T
0.5593493585379153 0.3062179211697987 0.3446299721340639 T T T
0.9500677745824935 0.2062959084272725 0.4938635907271290 T T T
0.1871616958115551 0.6311045091801255 0.3084528223475062 T T T
0.6281444068848134 0.4809309947240797 0.2966513782278707 T T T
0.9833850243052964 0.9187396555103425 0.4807878455946838 T T T
0.8345275938261286 0.2022990467232837 0.5340702030100596 T T T
0.8847105513087193 0.3979747675378431 0.2923987441860293 T T T
0.6390423314860627 0.3790025452074485 0.3911348466230582 T T T
0.5379072674622848 -0.0518562563988339 0.2663091462928762 T T T
0.2801760170614679 0.9123371322679282 0.4588618222645112 T T T
0.9160163607125077 0.5125010936354706 0.3547876811921072 T T T
0.9570076788259341 0.7699035828216076 0.3508027010917742 T T T
0.0151005392999445 0.2001833608567946 0.4155821023657319 T T T
0.3757971174254315 0.8315404317022068 0.3466716515998310 T T T
0.6017640044957381 0.7800379148824780 0.5103666758389067 T T T

0.6369628448149067 0.4353306430768728 0.4676700214821279 T T T
 0.3644979094895044 0.1469852390282753 0.4908567067056628 T T T
 0.1792216580105908 0.7159137717005841 0.2967652376646921 T T T
 0.2114686222221119 0.5392440708050267 0.5049113506682870 T T T
 0.2385221901125618 0.3249845460675045 0.4311555598644246 T T T
 0.6275359500880674 0.5493621463869185 0.2671762603886590 T T T
 0.0279469391850640 0.8503949501781662 0.4639220783529608 T T T
 0.6958976057355755 0.9873419964751372 0.4467311295923593 T T T
 0.9213477852307731 0.2173141177586712 0.5360735287452429 T T T
 0.8494405669457507 0.3272708093451180 0.2711399495159622 T T T
 0.6338276326372445 0.3533056244929355 0.3478312792542997 T T T
 0.2205492307279767 0.4402673385990477 0.2858101138633847 T T T
 0.4292612770751796 0.2227970684587979 0.2869992628689824 T T T
 0.2295326339907539 0.4328434728715311 0.2319685938906449 T T T
 0.4242783676322247 0.2293320000163509 0.2330428285767004 T T T

Transition state in the CO–CO coupling on Cu(100) surface at –1.0 V (vs. SHE)

1.00000000000000
 11.038299999999996 0.000000000000000 0.000000000000000
 0.000000000000000 11.038299999999996 0.000000000000000
 0.000000000000000 0.000000000000000 22.000000000000000

Cu H O C

54 36 20 2

Selective dynamics

Direct

0.166670000000034 0.000000000000000 0.000000000000000 F F F
 0.500000000000000 0.000000000000000 0.000000000000000 F F F
 0.833329999999965 0.000000000000000 0.000000000000000 F F F
 0.000000000000000 0.166670000000034 0.000000000000000 F F F
 0.333329999999966 0.166670000000034 0.000000000000000 F F F
 0.666670000000034 0.166670000000034 0.000000000000000 F F F
 0.166670000000034 0.333329999999966 0.000000000000000 F F F

0.5000000000000000	0.3333299999999966	0.0000000000000000	F F F
0.8333299999999965	0.3333299999999966	0.0000000000000000	F F F
0.0000000000000000	0.5000000000000000	0.0000000000000000	F F F
0.3333299999999966	0.5000000000000000	0.0000000000000000	F F F
0.6666700000000034	0.5000000000000000	0.0000000000000000	F F F
0.1666700000000034	0.6666700000000034	0.0000000000000000	F F F
0.5000000000000000	0.6666700000000034	0.0000000000000000	F F F
0.8333299999999965	0.6666700000000034	0.0000000000000000	F F F
0.0000000000000000	0.8333299999999965	0.0000000000000000	F F F
0.3333299999999966	0.8333299999999965	0.0000000000000000	F F F
0.6666700000000034	0.8333299999999965	0.0000000000000000	F F F
0.9998233766713227	0.0011801764286332	0.0805638479343287	T T T
0.3346025727223178	0.0016618656797363	0.0817547629602444	T T T
0.6656589298059146	0.9997947945225434	0.0815426773064089	T T T
0.1679812628257693	0.1689982829062870	0.0820310623625104	T T T
0.4995535834565671	0.1645770526200323	0.0814994240545772	T T T
0.8343077408565590	0.1696508731844233	0.0820134821625018	T T T
0.9992533486985735	0.3334394589934320	0.0827111169751333	T T T
0.3328498942381941	0.3331458042388959	0.0789066462231105	T T T
0.6665889747640961	0.3360943053171326	0.0841842561335895	T T T
0.1663252214647599	0.5013072296093455	0.0812233816751444	T T T
0.4990623591611723	0.4975530070846972	0.0834499032865494	T T T
0.8304981639523632	0.4978923949989564	0.0833340317537363	T T T
0.0021219395457095	0.6682498992253230	0.0813790833441459	T T T
0.3306292307397456	0.6654541014068087	0.0817653945198771	T T T
0.6664129377797536	0.6641995605053950	0.0817645061725329	T T T
0.1654198699314833	0.8332098008628037	0.0812758211037447	T T T
0.5008758706325409	0.8353396915515248	0.0813954387857976	T T T
0.8336111591481837	0.8339731791884545	0.0802125450820341	T T T
0.1656238709030688	0.9989809414510161	0.1622801733089005	T T T
0.5028758902629491	0.9936930682108381	0.1687382457184441	T T T
0.8339638293591918	0.0001826731851509	0.1624804126609262	T T T

0.0034002991382920	0.1628794168625802	0.1624760582242785	T	T	T
0.3309426684627255	0.1626374482709210	0.1650235473158119	T	T	T
0.6687378291938657	0.1645948702589947	0.1602909076449634	T	T	T
0.1626531151683395	0.3370874187136721	0.1663087830653964	T	T	T
0.4984064238627468	0.3254321176427553	0.1657068300078990	T	T	T
0.8367613046743186	0.3321920097145750	0.1703523137999596	T	T	T
0.9993159350840414	0.5044911317482388	0.1606064069472950	T	T	T
0.3297116986637789	0.5018009785053863	0.1645275470332947	T	T	T
0.6626609796342038	0.5036492393742336	0.1683503592565145	T	T	T
0.1631099875245923	0.6750403961584368	0.1682340683578971	T	T	T
0.4955452330308816	0.6706277252556490	0.1606106832025560	T	T	T
0.8371331828019847	0.6701254084985422	0.1613196114671780	T	T	T
0.9962884297194207	0.8387515948578042	0.1628028702688624	T	T	T
0.3317143497630184	0.8353702345327817	0.1604188090366207	T	T	T
0.6720226438169590	0.8311056160128132	0.1611845943974117	T	T	T
0.4602011603733728	0.9256540492639047	0.2894928634486788	T	T	T
0.9719816523653861	0.4692643740572819	0.3825910884736742	T	T	T
0.3201619726208733	0.8659607956559725	0.4817774674265251	T	T	T
0.9376562892876307	0.5874813971296433	0.3481686632384324	T	T	T
0.0340371984373462	0.1189234291399472	0.3957412395178891	T	T	T
0.9197796331330891	0.8039155258925987	0.3231310807226108	T	T	T
0.4336797485901727	0.7588752640127154	0.3494996143847970	T	T	T
0.0923013009573594	0.2432314542894929	0.4122371801206767	T	T	T
0.3109555427771795	0.7778922063703532	0.3154769558778482	T	T	T
0.6655159798275534	0.7216990961099867	0.5156340089560486	T	T	T
0.4465569587681628	0.1584001499412366	0.4846920642659640	T	T	T
0.7063951937539983	0.4501582578230625	0.4711604479953663	T	T	T
0.4814257069272898	0.0652986817499013	0.2843358738582395	T	T	T
0.3152363672915185	0.8843745701036454	0.4114737013287239	T	T	T
0.9983192928360153	0.7872213967620070	0.3823162470110261	T	T	T
0.5782183857833161	0.8043613117072965	0.5515687546210301	T	T	T
0.5959118859200956	0.3705137607751041	0.4878248034730603	T	T	T

0.3373535348727685	0.0740073371437191	0.4684903682688883	T	T	T
0.2274233112685593	0.4693571966370768	0.4726462209272881	T	T	T
0.2647547505267696	0.3517264552511890	0.3786554197364324	T	T	T
0.1094211210770197	0.7184340833260237	0.2969491120633378	T	T	T
0.2965058207225013	0.5639082279826795	0.5115010015761284	T	T	T
0.2889707285115932	0.2715481579036236	0.4370299414656457	T	T	T
0.6889731700773751	0.6072246175163798	0.2811506823996836	T	T	T
0.1181715526579339	0.8720675155138338	0.4549156150495861	T	T	T
0.6566091759986961	0.9156026317031659	0.4648210030133483	T	T	T
0.6280041338339899	0.0040966112375216	0.4119424740673736	T	T	T
0.7681184682991358	0.3127898377262213	0.2896259092184862	T	T	T
0.5527502521894050	0.3055258057669690	0.3314259972343833	T	T	T
0.9526123513770912	0.2062621168476042	0.4916322964978334	T	T	T
0.1986530965599300	0.6091100540962486	0.2887931695266914	T	T	T
0.6275034846236665	0.4806830236515509	0.2928325217395979	T	T	T
0.9833037725559635	0.9055677124687023	0.4687054823033491	T	T	T
0.8357580542462841	0.2061863987949693	0.5307685784634372	T	T	T
0.8845778664740536	0.3899120424403861	0.2913954812846668	T	T	T
0.6285696671021554	0.3726015637317061	0.3821129716570297	T	T	T
0.5118191752693733	0.9874036590571151	0.2692801571696108	T	T	T
0.2834170203773496	0.9163367512592941	0.4503637454056530	T	T	T
0.9162113251967482	0.5011597816234143	0.3523360555331009	T	T	T
0.9800828120137126	0.7511625622990862	0.3416617842018538	T	T	T
0.0151130099855550	0.1978272226840545	0.4130091147341587	T	T	T
0.3756993480810067	0.8213450482192997	0.3377305125669849	T	T	T
0.6006069037300037	0.7805822904512354	0.5104040968053524	T	T	T
0.6252000047171578	0.4281475093011764	0.4576864656134276	T	T	T
0.3586930287938301	0.1572405017727263	0.4810232866524799	T	T	T
0.1852428780753854	0.6930473689578561	0.2758028904532068	T	T	T
0.2151230020808939	0.5372812002189845	0.5010185873889837	T	T	T
0.2337017388530782	0.3332448196301740	0.4191199647699050	T	T	T
0.6291650219661022	0.5513799613566022	0.2645483726223787	T	T	T

0.0348585464648536	0.8392963507945055	0.4551063945690003	T	T	T
0.6898977769422103	0.9847836032098555	0.4418881031350352	T	T	T
0.9229947134705866	0.2174069813935517	0.5336572146765589	T	T	T
0.8470254958386221	0.3213619923383888	0.2691538440032559	T	T	T
0.6280584934173490	0.3500027454866057	0.3383151296828685	T	T	T
0.2422916602347129	0.4338055464965009	0.2872795825965397	T	T	T
0.4153151809462443	0.2311965430167149	0.2870768911253449	T	T	T
0.2665367900614015	0.4025792527857277	0.2357021824437737	T	T	T
0.3918902950940505	0.2628997116821381	0.2352356904734804	T	T	T

References

- (1) Kresse, G.; Furthmüller, J. Efficient iterative schemes for ab initio total-energy calculations using a plane-wave basis set. *Physical Review B* **1996**, *54* (16), 11169-11186.
- (2) Kresse, G.; Furthmüller, J. Efficiency of ab-initio total energy calculations for metals and semiconductors using a plane-wave basis set. *Computational Materials Science* **1996**, *6* (1), 15-50.
- (3) Hammer, B.; Hansen, L. B.; Nørskov, J. K. Improved adsorption energetics within density-functional theory using revised Perdew-Burke-Ernzerhof functionals. *Physical Review B* **1999**, *59* (11), 7413-7421.
- (4) Trasatti, S. The absolute electrode potential: an explanatory note (Recommendations 1986). *Journal of Electroanalytical Chemistry and Interfacial Electrochemistry* **1986**, *209* (2), 417-428.
- (5) Hjorth Larsen, A.; Jørgen Mortensen, J.; Blomqvist, J.; Castelli, I. E.; Christensen, R.; Dułak, M.; Friis, J.; Groves, M. N.; Hammer, B.; Hargus, C.; et al. The atomic simulation environment—a Python library for working with atoms. *Journal of Physics: Condensed Matter* **2017**, *29* (27), 273002.
- (6) Chen, B. W. J.; Zhang, X.; Zhang, J. Accelerating explicit solvent models of heterogeneous catalysts with machine learning interatomic potentials. *Chemical Science* **2023**, *14* (31), 8338-8354.
- (7) Podryabinkin, E. V.; Shapeev, A. V. Active learning of linearly parametrized interatomic potentials. *Computational Materials Science* **2017**, *140*, 171-180.
- (8) Shapeev, A. V. Moment Tensor Potentials: A Class of Systematically Improvable Interatomic Potentials. *Multiscale Modeling & Simulation* **2016**, *14* (3), 1153-1173.
- (9) Novikov, I. S.; Gubaev, K.; Podryabinkin, E. V.; Shapeev, A. V. The MLIP package: moment tensor potentials with MPI and active learning. *Machine Learning: Science and Technology* **2021**, *2* (2), 025002.
- (10) Henkelman, G.; Jónsson, H. A dimer method for finding saddle points on high dimensional potential surfaces using only first derivatives. *The Journal of Chemical Physics* **1999**, *111* (15), 7010-7022.
- (11) Henkelman, G.; Uberuaga, B. P.; Jónsson, H. A climbing image nudged elastic band method for finding saddle points and minimum energy paths. *The Journal of Chemical Physics* **2000**, *113* (22), 9901-9904.